Inorg. Chem. **2006**, *45*, 7973–7980

$Cu_2\{[18]ane\text{-}N_6\}$ Complexes: Structures, Magnetism, and Phosphate Monoester Binding

Julia E. Barker,[†] Yu Liu,[†] Gordon T. Yee,[‡] Wei-Zhong Chen,[†] Guangbin Wang,[‡] Vilma M. Rivera,[†] and Tong Ren*[,†,§]

Department of Chemistry, University of Miami, Coral Gables, Florida 33124, Department of Chemistry, Virginia Polytechnic Institute and State University, Blacksburg, Virginia 24061, and Department of Chemistry, Purdue University, West Lafayette, Indiana 47907

Received June 20, 2006

A novel Cu^{II}_2 complex of the [18]ane-N_6 macrocycle ([18]ane-N_6 = 1,4,7,10,13,16-hexaazacyclooctadecane) was prepared from the reaction between [18]ane-N_6 and Cu^{II} salts such as $Cu(NO_3)_2$ and $Cu(OAc)_2$. A structural study of the complex derived from $Cu(OAc)_2$ (**1**) revealed a Cu^{II}_2 core encircled by a [18]ane-N_6 ligand and two μ-O-OAc ligands. The facile replacement of μ-O-OAc by a phosphate monoester $[PO_3(OR)^{2-}]$ yielded a number of bis(phosphate monoester)dicopper complexes with $ROPO_3^{2-}$ as hydrogen phosphate (HPO_4^{2-}, **3a**), phenyl phosphate $[PO_3(OPh)^{2-}$, **3b**], glycerol 2-phosphate $[PO_3(OCH(CH_2OH)_2)^{2-}$, **3c**], α-D-gluocose phosphate $[PO_3(C_6H_{11}O_6)^{2-}$, **3d**], and DL-α-glycerol phosphate $[PO_3(OCH_2CHOHCH_2OH)^{2-}$, **3e**]. Structural studies of compounds **3a**–**d** confirmed both the retention of the $Cu_2\{[18]ane\text{-}N_6\}$ core and a μ-O-PO_3(OR) coordination mode. Displacement of acetate by a phosphate monoester in an aqueous solution was accompanied by a significant change in the visible absorption, which enables the establishment of relative association constants of $PO_3(OR)^{2-}$ on the order of 10^4 in the unbuffered solution and 10^3 in the buffered solution (HEPES). Measurement of the magnetic susceptibility of compound **3a** over the temperature range of 5–300 K and subsequent modeling revealed a weak antiferromagnetic coupling ($J = -1.1$ cm^{-1}) between two Cu^{II} centers.

Introduction

Phosphate-containing species are among the most important molecules in the biosphere because they are the building blocks of nucleic acids, intermediary metabolites, and energy storage units.[1] For this reason, recognition and binding of phosphate anions have drawn sustained interest from both chemists and structural biologists. The importance of aza-crown ethers in phosphate recognition and phosphoryl transfer is underscored by both the landmark study of Lehn[2,3] and many other follow-up studies.[4] A notable example among the latter is 1,4,7,10,13,16-hexaazacyclooctadecane ([18]ane-N_6), which was shown to bind two dihydropyrophosphates ($H_2P_2O_7^{2-}$) at pH = 3 by Bencini and co-workers[5] and various equivalents of dihydrophosphate ($H_2PO_4^-$) or hydrophosphate (HPO_4^{2-}) depending on the pH (ranging from 1 to 8) by Spiccia and co-workers.[6] Binding of other anions such as Cl^-, Br^-, I^-/I_3^-, $CF_3SO_3^-$, HSO_4^-/SO_4^{2-}, and $Co(CN)_6^{3-}$ by [18]ane-N_6 have also been reported.[7] The presence of six secondary amine centers in neutral [18]ane-

* To whom correspondence should be addressed. E-mail: tren@purdue.edu.
† University of Miami.
‡ Virginia Polytechnic Institute and State University.
§ Purdue University.

(1) Westheimer, F. H. *Science* **1987**, *235*, 1173. Westheimer, F. H. *ACS Symp. Ser.* **1992**, *486*, 1.
(2) Hosseini, M. W.; Lehn, J. M.; Mertes, M. P. *Helv. Chim. Acta* **1983**, *66*, 2454. Hosseini, M. W.; Lehn, J. M.; Maggiora, L.; Mertes, K. B.; Mertes, M. P. *J. Am. Chem. Soc.* **1987**, *109*, 537. Hosseini, M. W.; Lehn, J. M. *J. Am. Chem. Soc.* **1987**, *109*, 7047. Hosseini, M. W.; Lehn, J. M.; Jones, K. C.; Plute, K. E.; Mertes, K. B.; Mertes, M. P. *J. Am. Chem. Soc.* **1989**, *111*, 6330. Hosseini, M. W.; Blacker, A. J.; Lehn, J. M. *J. Am. Chem. Soc.* **1990**, *112*, 3896.
(3) Lehn, J.-M. *Supramolecular Chemistry*; VCH: Weinheim, Germany, 1995.
(4) Bianchi, A.; Bowman-James, K.; García-España, E. *Supramolecular Chemistry of Anions*; Wiley-VCH: New York, 1997.
(5) Bazzicalupi, C.; Bencini, A.; Bianchi, A.; Cecchi, M.; Escuder, B.; Fusi, V.; Garcia-Espana, E.; Giorgi, C.; Luis, S. V.; Maccagni, G.; Marcelino, V.; Paoletti, P.; Valtancoli, B. *J. Am. Chem. Soc.* **1999**, *121*, 6807.
(6) Warden, A. C.; Warren, M.; Hearn, M. T. W.; Spiccia, L. *Inorg. Chem.* **2004**, *43*, 6936.
(7) Warden, A. C.; Warren, M.; Hearn, M. T. W.; Spiccia, L. *New J. Chem.* **2004**, *28*, 1160. Warden, A. C.; Warren, M.; Hearn, M. T. W.; Spiccia, L. *New J. Chem.* **2004**, *28*, 1301. Cullinane, J.; Gelb, R. I.; Margulis, T. N.; Zompa, L. J. *J. Am. Chem. Soc.* **1982**, *104*, 3048. Thuery, P.; Keller, N.; Lance, M.; Vigner, J. D.; Nierlich, M. *Acta Crystallogr., Sect. C: Cryst. Struct. Commun.* **1995**, *51*, 1407.

10.1021/ic0611140 CCC: $33.50
Published on Web 08/23/2006

Chart 1. Two Observed Coordination Modes of [18]ane-N_6

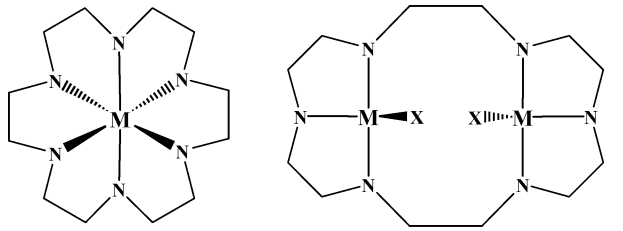

(a) Pseudooctahedral (b) binuclear square planar

N_6 makes it an ideal ligand for transition-metal ions, and indeed complex ions of Cr^{3+}, Co^{2+}, Ni^{2+}, Pd^{2+}, Cu^{2+}, Zn^{2+}, and Hg^{2+} can be readily formed in an aqueous solution.[8] However, the coordination modes of [18]ane-N_6 are quite mundane: either a six-coordinate mononuclear binding mode (Chart 1), as in the cases of Co^{3+},[9] Hg^{2+},[10] and Cr^{3+},[11] or two tridentate chelating halves, with each supporting a Pd^{2+} center.[12] Mononuclear lanthanide/actinide complexes supported by [18]ane-N_6 are also known with M = U, Nd, and Er.[13]

Anion receptors with high affinity and selectivity are currently topical.[4,14] Intense efforts have been focused on organic receptors based on polyaza macrocycles, azacryptands, and polypyrroles, where high binding constants for phosphate were realized.[3,15] While many receptors exhibit high binding constants for phosphate anions in organic media, affinities tend to diminish in an aqueous solution. Hence, a great challenge remains to create receptors with high affinity and selectivity in an aqueous solution at physiological pH. Recently, the laboratories of Han and Kim[16] and Anslyn and co-workers[17] reported dinuclear Zn^{2+} and mononuclear Cu^{2+} complexes that bind HPO_4^{2-} with both high *affinity* and *selectivity* in an aqueous solution, demonstrating the great promise of metalloreceptors in phosphate recognition.

We communicated previously the synthesis of a Cu^{II}_2 complex supported by a single [18]ane-N_6 (**1**, Scheme 1), which is unique in coordination geometry, and the high association constants of various phosphate monoesters [$PO_3(OR)^{2-}$] toward **1** in an aqueous solution.[18] Reported in this contribution are (i) the detailed synthesis of **1**, its carbonato analogue **2**, and the phosphate monoester derivatives **3**; (ii) structural elucidation of complexes **1**−**3** and their relevance to the active sites of metallophosphatases; (iii) the relative binding strength of phosphate monoester to the {[18]ane-N_6}Cu_2 unit; and (iv) the spin coupling between two Cu^{II} centers.

Scheme 1. Synthesis of Cu_2{[18]ane-N_6} Complexes[a]

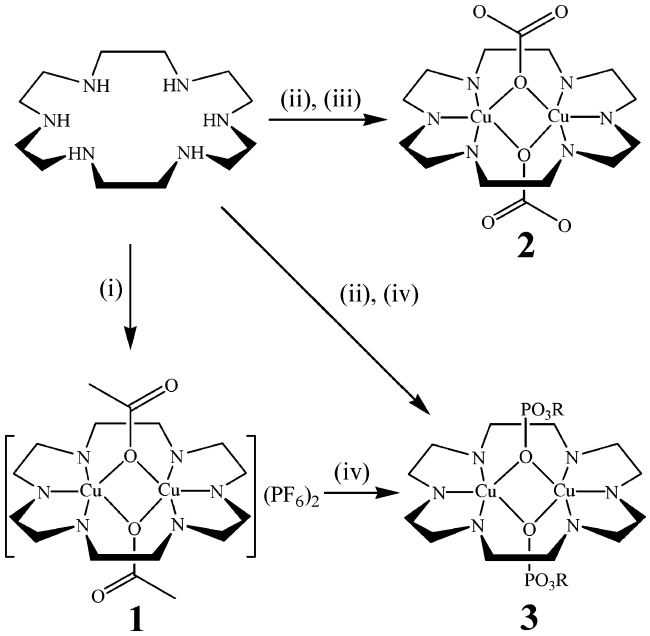

[a] (i) 2 equiv of $Cu(OAc)_2$, KPF_6; (ii) 2 equiv of $Cu(NO_3)_2$; (iii) 3 equiv of K_2CO_3; (iv) 2 equiv of Na_2PO_4R, where R = H (**3a**), Ph (**3b**), $CH(CH_2OH)_2$ (**3c**), $C_6H_{11}O_6$ (**3d**), and $CH_2CHOHCH_2OH$ (**3e**).

Results and Discussion

Synthesis. It was discovered early in our study that aqueous [18]ane-N_6 reacted readily with various Cu^{II} salts including $Cu(NO_3)_2$ and $Cu(OAc)_2$ to yield royal-blue solutions. While the species resulting from the addition of $Cu(NO_3)_2$ has not been crystallized, that from $Cu(OAc)_2$ was easily crystallized upon the addition of KPF_6. Single-crystal X-ray diffraction analysis revealed the compound as {Cu_2-(μ-O-OAc)$_2$([18]ane-N_6)}$(PF_6)_2$ (**1**). Although the exact nature of the species derived from the addition of $Cu(NO_3)_2$ remains elusive, it is likely a dinuclear species and served as a convenient starting material: the addition of K_2CO_3 to this intermediate solution resulted in a neutral Cu_2 species Cu_2(μ-O-CO_3)$_2$([18]ane-N_6) (**2**). The feature of μ-O acetate in **1** (see the discussion below) makes the Cu_2{[18]ane-N_6} scaffold an attractive receptor for other oxy anions, especially phosphate esters. The feasibility was confirmed by the darkening of aqueous **1** upon the addition of the salt of phosphate monoesters, and the reaction of **1** with 3−4 equiv of the salt of $PO_3(OR)^{2-}$ resulted in the formation of Cu_2-(μ-O-PO_3(OR))$_2$([18]ane-N_6) in satisfactory yield (**3a**−**c**, Scheme 1). Cu_2(μ-O-PO_3(OR))$_2$([18]ane-N_6)-type compounds can also be directly prepared from aqueous [18]ane-N_6 via

(8) Mitewa, M.; Bontchev, P. R. *Coord. Chem. Rev.* **1994**, *135*, 129.
(9) Royer, D. J.; Grant, G. J.; Derveer, D. G. V.; Castillo, M. J. *Inorg. Chem.* **1982**, *21*, 1902. Yoshikawa, Y.; Toriumi, K.; Ito, T.; Yamatera, H. *Bull. Chem. Soc. Jpn.* **1982**, *55*, 1422. Morooka, M.; Ohba, S.; Toriumi, K. *Acta Crystallogr., Sect. B: Struct. Sci.* **1992**, *48*, 459.
(10) Carrondo, M. A. A. F. d. C. T.; Félix, V.; Duarte, M. T.; Santos, M. A. *Polyhedron* **1993**, *12*, 931.
(11) Chandrasekhar, S.; Fortier, D. G.; McAuley, A. *Inorg. Chem.* **1993**, *32*, 1424.
(12) Bencini, A.; Bianchi, A.; Dapporto, P.; Garciaespana, E.; Micheloni, M.; Paoletti, P.; Paoli, P. *J. Chem. Soc., Chem. Commun.* **1990**, 1382. McAuley, A.; Whitcombe, T. W.; Zaworotko, M. J. *Inorg. Chem.* **1991**, *30*, 3513.
(13) Nierlich, M.; Sabattie, J. M.; Keller, N.; Lance, M.; Vigner, J. D. *Acta Crystallogr., Sect. C: Cryst. Struct. Commun.* **1994**, *50*, 52. Bu, X. H.; Lu, S. L.; Zhang, R. H.; Wang, H. G.; Yao, X. K. *Polyhedron* **1997**, *16*, 3247. Wang, R. Y.; Zhao, J. J.; Jin, T. Z.; Xu, G. X.; Zhou, Z. Y.; Zhou, X. G. *Polyhedron* **1998**, *17*, 43.
(14) Gale, P. A. *Coord. Chem. Rev.* **2003**, *240*, 3. Stibor, I., Ed. *Anion Sensing*; Springer: Berlin, 2005.
(15) Sessler, J. L.; Camiolo, S.; Gale, P. A. *Coord. Chem. Rev.* **2003**, *240*, 17. Beer, P. D.; Gale, P. A. *Angew. Chem., Int. Ed.* **2001**, *40*, 486.
(16) Han, M. S.; Kim, D. H. *Angew. Chem., Int. Ed.* **2002**, *41*, 3809.
(17) Tobey, S. L.; Anslyn, E. V. *Org. Lett.* **2003**, *5*, 2029. Tobey, S. L.; Jones, B. D.; Anslyn, E. V. *J. Am. Chem. Soc.* **2003**, *125*, 4026.
(18) Barker, J. E.; Liu, Y.; Martin, N. D.; Ren, T. *J. Am. Chem. Soc.* **2003**, *125*, 13332.

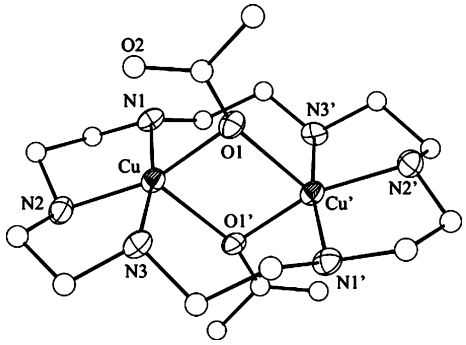

Figure 1. ORTEP plot of $[\mathbf{1}]^{2+}$ at the 30% probability level. H atoms were omitted for clarity.

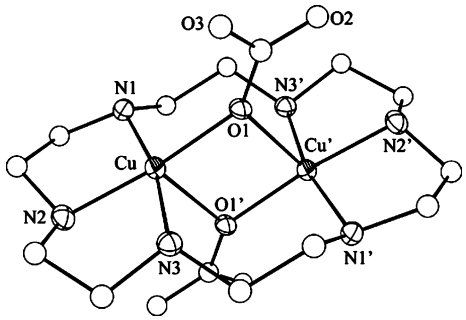

Figure 2. ORTEP plot of molecule **2** at the 30% probability level. H atoms were omitted for clarity.

Table 1. Selected Bond Lengths (Å) and Angles (deg) for Compounds **1**, **2**, **3a**, and **3b**

	1	**2**	**3a**	**3b**
Cu−O1	2.009(3)	1.958(3)	1.978(3)	1.926(3)
Cu−O1′	2.249(3)	2.227(3)	2.202(3)	2.306(3)
Cu−N1	2.068(9)	2.067(3)	2.034(4)	2.022(4)
Cu−N2	1.990(3)	1.992(4)	1.997(4)	1.960(4)
Cu−N3	1.985(10)	2.056(3)	2.061(4)	2.032(5)
P−O1			1.547(3)	1.524(3)
Cu···Cu′	3.1158(8)	3.134(1)	3.036(1)	2.972(1)
Cu−O1−Cu′	93.9(1)	96.8(1)	93.0(1)	88.8(1)
O1−Cu−O1′	86.1(1)	83.2(1)	87.0(1)	91.2(1)
P−O1−Cu			127.0(2)	135.5(2)
P−O1−Cu			139.1(2)	135.3(2)

$Cu(NO_3)_2$ in a single step, as demonstrated with the synthesis of compound **3d**. Compound **3e** was generated in situ through the titration of **1** by disodium DL-α-glycerol phsphate (see the Spectroscopic Titrations section) but not isolated.

Molecular Structures. Compounds **1**−**3** readily crystallized from aqueous solutions, and molecular structures of compounds **1**−**3** were determined using single-crystal X-ray diffraction analysis. Structural plots of the cations of compound **1** and molecule **2** are shown in Figures 1 and 2, respectively, and their selected bond lengths and angles are listed in Table 1. It is clear from Figure 1 that the bulk of $[\mathbf{1}]^{2+}$ is a ruffled rectangle consisting of the [18]ane-N_6 ring and two Cu^{II} ions encircled, and the latter are bridged by two μ-O acetates above and beneath the rectangle. Two Cu^{II} centers within the same cation are related by a crystallographic inversion center and, consequently, have identical topological features. The coordination sphere of the Cu center is best described as distorted square-pyramidal, where the basal ligand centers are O1, N1, N2, and N3 and the apical ligand center is O1′. The apical Cu−O1′ bond is significantly longer than the basal bonds, which is typical for square-pyramidal Cu^{II} species.[19] In the majority of [18]ane-N_6 complexes reported thus far, the macrocycle supports a single metal center (M) in the hexadentate mode with M as Co^{3+}, Cr^{3+}, Hg^{2+}, $(UO_2)^{2+}$, Nd^{3+}, and Er^{3+}.[8−11,13] In the only dinuclear example, the [18]ane-N_6 ligand supports two noninteracting Pd^{2+} centers.[12] Hence, cation **1** represents a novel coordination motif of the [18]ane-N_6 macrocycle.

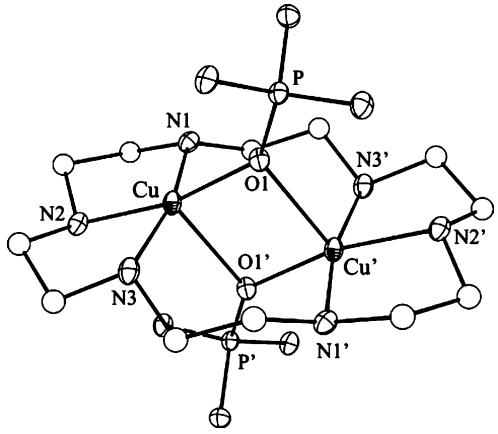

Figure 3. ORTEP plot of molecule **3a** at the 30% probability level. H atoms were omitted for clarity.

Similar to compound **1**, the carbonate-bridged compound **2** (Figure 2) exhibits the square-pyramidal Cu^{II} center of an elongated apical bond. It is noted that the Cu−O1 and Cu−O1′ bond lengths in **2** are slightly shortened from those in **1**, reflecting the increased donor strength of CO_3^{2-} over OAc^-. Di- and polynuclear Cu complexes of carbonato bridges are known,[20] and these species may be relevant to CO_2 sequestering.[21]

Molecular structures of phosphate monoester compounds **3a**−**d** are shown in Figures 3−6. Similar to compounds **1** and **2**, both **3a** and **3b** have a crystallographic inversion center that relates half of the molecule to the other, and their metric parameters are, hence, listed along with those of **1** and **2** in Table 1. It is clear from Figure 3 that the displacement of μ-OAc by HPO_4^{2-} does not change the overall feature of the Cu_2{[18]ane-N_6} moiety and each Cu^{2+} center retains the square-pyramidal coordination geometry. Both the Cu−O1 (basal) and Cu−O1′ (apical) bond lengths are comparable to those of **2** because the μ-O species are dianions in both cases. Compound **3b** exhibits a further shortened basal Cu−O bond and an elongated apical Cu−O bond, which are consistent with the enhanced donor strength of phosphate monoester compared with that of μ-OAc.

Glycerol phosphates are important participants of the synthesis and degradation of phospholipids. Despite their significance in the biosphere, structural understandings of

(19) Hathaway, B. J. Copper. In *Comprehensive Coordination Chemistry*; Wilkinson, G., Ed.; Pergamon Press: New York, 1987. Liu, Y.; Ren, T. *Inorg. Chim. Acta* **2003**, *348*, 279.

(20) Darensbourg, D. J.; Holtcamp, M. W.; Khandelwal, B.; Reibenspies, J. H. *Inorg. Chem.* **1995**, *34*, 5390. Youngme, S.; Chaichit, N.; Kongsaeree, P.; Albada, G. A. v.; Reedijk, J. *Inorg. Chim. Acta* **2001**, *324*, 232. Fernandes, C.; Neves, A.; Bortoluzzi, A. J.; Szpoganicz, B.; Schwingel, E. *Inorg. Chem. Commun.* **2001**, *4*, 354.

(21) Newell, R.; Appel, A.; DuBois, D. L.; DuBois, M. R. *Inorg. Chem.* **2005**, *44*, 365.

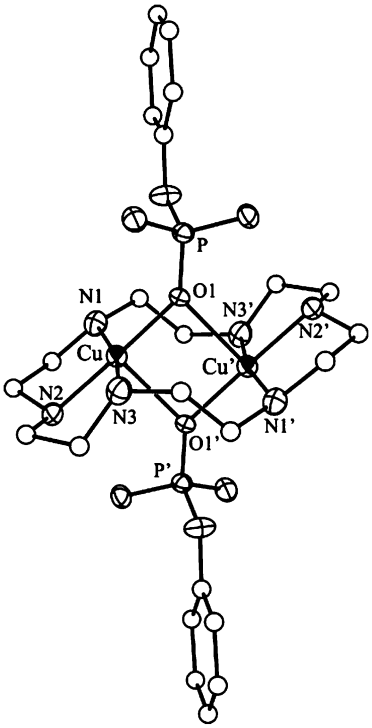

Figure 4. ORTEP plot of molecule **3b** at the 30% probability level. H atoms were omitted for clarity.

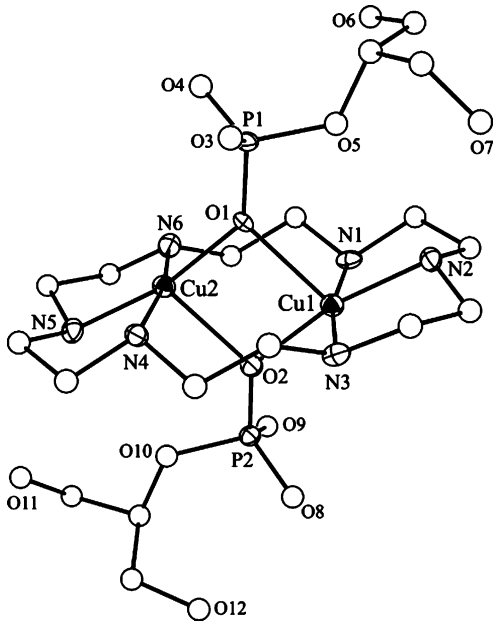

Figure 5. ORTEP plot of molecule **3c** at the 30% probability level. H atoms were omitted for clarity.

both α- and *β*-glycerol phosphates are limited to the studies of their Na_2 salts.[22] The structural study of **3c** is the first for coordination compounds of *β*-glycerol phosphate (2-GP) to our knowledge. The asymmetric unit of **3c** contains one Cu_2-(μ-O-2-GP)$_2$([18]ane-N_6) molecule. The two crystallographically inequivalent Cu centers have the same type of square-pyramidal geometry and comparable bond lengths and angles in their first coordination sphere. The latter metrical parameters, listed in Table 2, are also similar to those of compounds **3a** and **3c**. Similar to the structure of the Na_2 salt of 2-GP,[22] both phosphate moieties display long P−O(ester) bonds [1.623(7) and 1.620(7) Å]. The P−O(free) bond lengths (1.49−1.52 Å) are significantly longer than that of a typical P═O bond (1.43 Å) and indicative of delocalized charge. As expected, P−O(−Cu) bonds (ca. 1.55 Å) are significantly longer than P−O(free) bonds because of coordination to Cu centers.

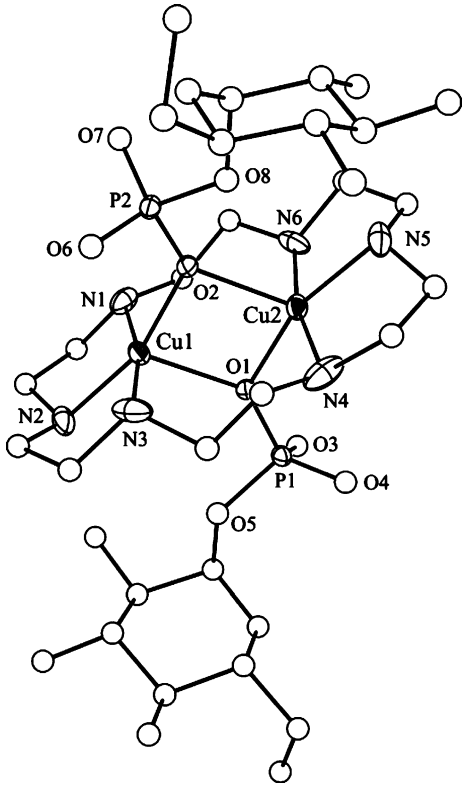

Figure 6. ORTEP plot of molecule **3d** at the 30% probability level. H atoms were omitted for clarity.

Table 2. Selected Bond Lengths (Å) and Angles (deg) for Compounds **3c** and **3d**

	3c	**3d**
Cu1−O1	2.253(6)	2.175(5)
Cu1−O2	1.967(6)	1.982(5)
Cu2−O1	1.961(6)	1.975(5)
Cu2−O2	2.233(6)	2.178(5)
Cu1−N1	2.052(7)	2.018(9)
Cu1−N2	2.004(8)	1.977(8)
Cu1−N3	2.062(8)	2.042(9)
Cu2−N4	2.034(8)	2.041(9)
Cu2−N5	1.982(9)	1.977(8)
Cu2−N6	2.049(8)	2.018(9)
P1−O1	1.549(6)	1.538(5)
P1−O3	1.506(7)	1.529(6)
P1−O4	1.497(7)	1.494(6)
P1−O5	1.623(7)	1.622(5)
P2−O2	1.552(7)	1.534(5)
P2−O6	1.518(7)	1.528(6)
P1−O7	1.487(7)	1.492(6)
P1−O8	1.620(7)	1.622(5)
Cu1···Cu2	3.088(2)	2.985(1)
Cu1−O1−Cu2	94.0(2)	91.8(2)
Cu1−O2−Cu2	94.5(2)	91.6(2)
P1−O1−Cu1	131.3(3)	139.0(3)
P1−O1−Cu2	134.6(4)	126.9(3)
P2−O2−Cu1	132.9(4)	139.0(3)
P2−O2−Cu2	132.3(4)	126.9(3)

(22) Taga, T.; Senma, M.; Osaki, K. *J. Chem. Soc., Chem. Commun.* **1972**, 465. Ul-Haque, M.; Caughlan, C. N. *J. Am. Chem. Soc.* **1966**, *88*.

The molecular structure of compound **3d** is shown in Figure 6, and its similarity to other Cu_2{[18]ane-N_6} moieties in terms of Cu coordination is obvious from both the ORTEP plot and geometric parameters listed in Table 2. The noteworthy feature of **3d** is the incorporation of α-D-glucose phosphate (α-D-Glc-1P). Structurally defined coordination compounds of α-D-Glc-1P are sparse despite the importance of α-D-Glc-1P in the biosphere. In addition to the alkali salts,[23] there has been only one report of transition-metal complexes of α-D-Glc-1P by the laboratory of Tanase, where four LCu^{II} units (L = bipy or phen) were linked with two α-D-Glc-1P ligands through both μ-O and μ-O,O′ coordination modes.[24] Similar to compounds **3a**−**d**, Tanase's complexes contain Cu^{II} centers in square-pyramidal geometry exclusively.

Scheme 2. Two-Metal-Ion Mechanism of Activation of Phosphate Diester

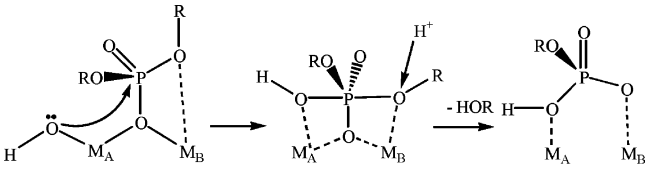

Topological features about compounds **3a**−**d** are relevant to the mechanistic understanding of bi/polymetallic phosphate esterases, for which a two-metal-ion model (Scheme 2) put forward by Steitz and Steitz has gained wide acceptance in recent years.[25,26] Because the μ-O mode depicted for **I** has not been identified in biological systems, structural insight into phosphate ester activation by metal centers has been extrapolated from a limited number of model studies, notably those of Cu^{2+} and Ni^{2+} complexes of phosphate *diesters* by Lippard and He.[27,28] For the purpose of comparison, selected metrical parameters around M_2(μ-*O*-phosphate) determined for Cu^{2+} and Ni^{2+} complexes of Lippard and compounds **3** are collected in Table 3.

Table 3. Selected Bond Lengths (Å) and Angles (deg) from Structures of Cu_2(μ-O-PO_4Ph_2),[27] Ni_2(μ-O-PO_4Ph_2)$_2$,[28] and Compounds **3**

	Cu_2(μ-O-PO_4Ph_2)	Ni_2(μ-O-PO_4Ph_2)$_2$	**3a**−**d**
$M-O_{short}$	2.235	2.129	1.93−1.98
$M-O_{long}$	2.397	2.142	2.18−2.31
P−O	1.489	1.51/1.52	1.52−1.55
M_A-M_B	3.09	3.134	2.97−3.09
M_A-O-M_B	107.49	94.1/94.4	88.8−94.5
$P-O-M_A$	120.50	124−130	126.9−139.0
$P-O-M_B$	152.40		126.9−139.0

In the Ni^{II}_2 complex by Lippard, each Ni center exhibits pseudooctahedral coordination geometry, and the bridging O centers are symmetrically positioned between two Ni centers. Similar to compounds **3** studied herein, the Cu^{II}_2 complex by Lippard has both Cu centers in square-pyramidal geometry and an unsymmetrical μ-O phosphate bridge. Compounds **3** have distinctly shorter M−O bonds than those found for Lippard's complexes, which is attributed to the higher charge of phosphate monoesters than that of diesters. The most notable feature of the two-metal-ion model by Steitz and Steitz is the optimal distance of 3.9 Å between two divalent metal ions, a structural fixture found for phosphatases/polymerases of separate evolutionary origins.[25] However, the M−M separations found for both Lippard's complexes and compounds **3** are much shorter. The discrepancy can be reconciled partially based on the difference in covalent radii among M^{II} centers: those of Cu^{II} (1.17 Å) and Ni^{II} (1.15 Å) are significantly smaller than those of Mg^{II} (1.36 Å) and Zn^{II} (1.25 Å), two ions typically found in phosphatases/polymerases.

Magnetic Interaction in Compounds 3. Spin-exchange interaction between two Cu^{II} centers is one of the most studied subjects in molecular magnetism. To examine the ability of μ-O phosphate in mediating magnetic interactions between two Cu^{II} centers in type **3** compounds, the magnetic susceptibility data for compound **3a** were recorded over the temperature range of 5−300 K (Figure 7). The χT vs T data can be modeled by a nonlinear least-squares fit[29] to the Bleaney−Bowers expression assuming a Hamiltonian of the form $H = -2J\mathbf{S}_1\cdot\mathbf{S}_2$:[30]

$$\chi T = \frac{2Ng^2\mu_B^2}{k}[3 + \exp(-2J/kT)]^{-1} \qquad (1)$$

where N, μ_B, and k have their usual meanings. This yields $g = 2.17 \pm 0.01$ and $J/k = -1.57 \pm 0.02$ K (or -1.1 cm^{-1}), indicating rather weak antiferromagnetic coupling between the two Cu^{2+} centers as mediated by the μ-O phosphate bridge.

It is interesting to wonder if the coupling is weak because the μ-O phosphate bridge is intrinsically weak or if this complex happens to have a geometry that is coincidentally near the crossover point between ferro- and antiferromagnetic coupling as seen in bridging dihydroxide species examined by Hatfield and co-workers.[31] In those complexes, a strong structure−property relationship was observed between the Cu−O−Cu bond angle and the strength and sign of the exchange interaction. It was noted in the paper of Hatfield and co-workers that $2J$ values range from +172 to −509 cm^{-1}, correlate linearly with the bond angle, and are about zero at approximately 97.5°. Should the same relationship be applicable to μ-O phosphate complexes, a rather strong ferromagnetic coupling in **3a** would be expected. The

(23) Beevers, C. A.; Maconoch, Gh. *Acta Crystallogr.* **1965**, *18*, 232. Narendra, N.; Seshadri, T. P.; Viswamitra, M. A. *Acta Crystallogr., Sect. C: Cryst. Struct. Commun.* **1984**, *40*, 1338.
(24) Kato, M.; Tanase, T. *Inorg. Chem.* **2005**, *44*, 8.
(25) Steitz, T. A.; Steitz, J. A. *Proc. Natl. Acad. Sci. U.S.A.* **1993**, *90*, 6498.
(26) Steitz, T. A. *J. Biol. Chem.* **1999**, *274*, 17395. Takagi, Y.; Warashina, M.; Stec, W. J.; Yoshinari, K.; Taira, K. *Nucleic Acids Res.* **2001**, *29*, 1815. Fedor, M. J. *Curr. Opin. Struct. Biol.* **2002**, *12*, 289. Nowotny, M.; Gaidamakov, S. A.; Crouch, R. J.; Yang, W. *Cell* **2005**, *121*, 1005.
(27) He, C.; Lippard, S. J. *J. Am. Chem. Soc.* **2000**, *122*, 184.
(28) He, C.; Gomez, V.; Spingler, B.; Lippard, S. J. *Inorg. Chem.* **2000**, *39*, 4188.
(29) Pezzullo, J. C. *Nonlinear Least Squares Regression (Curve Fitter)*, http://statpages.org/nonlin.html, 2005.
(30) Carlin, R. L. *Magnetochemistry;* Springer-Verlag: Berlin, 1986.
(31) Crawford, V. H.; Richardson, H. W.; Wasson, J. R.; Hodgson, D. J.; Hatfield, W. E. *Inorg. Chem.* **1976**, *15*, 2107.

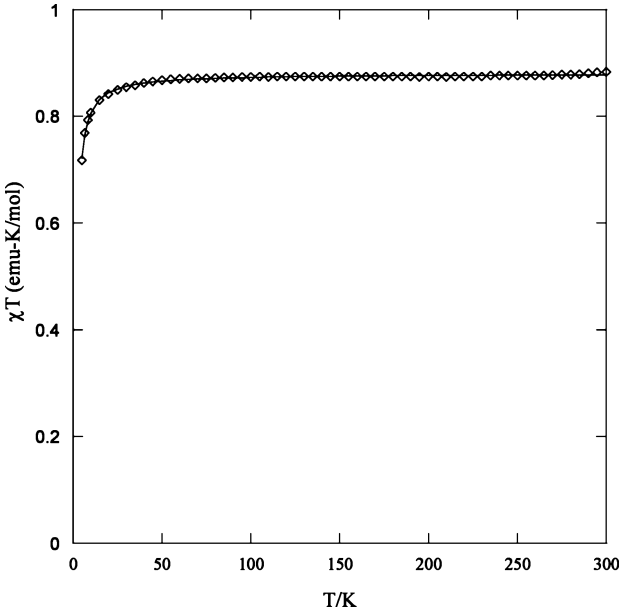

Figure 7. Measured χT values (open diamonds) and the least-squares fitting (solid line) derived from the Bleaney−Bowers equation.

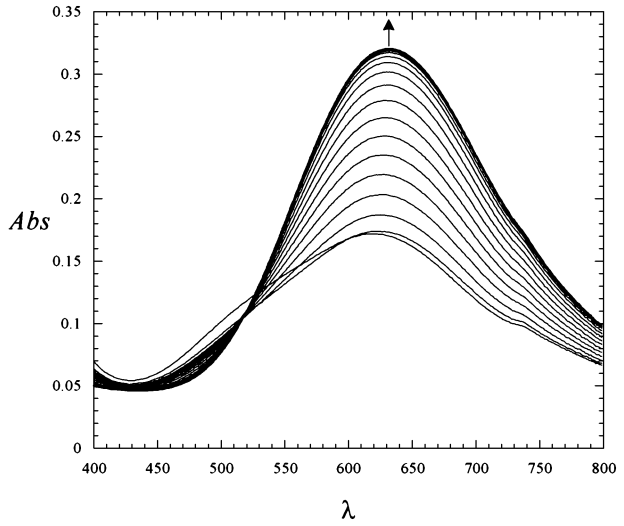

Figure 8. Spectroscopic titration of **1** by $Na_2$2-GP.

asymmetric nature of μ-O phosphate in compound **3a** may also contribute to the weak magnetic coupling. The answer to this question, we must await more magnetic data on μ-O phosphate complexes. All other phosphate-bridging Cu complexes for which a spin coupling constant (J) has been determined are μ-O,O′ phosphate based,[32] which precludes a meaningful comparison.

Spectroscopic Titrations. As noted early, the aqueous solution of compound **1** darkens with the addition of phosphate monoesters. This observation is easily understood from a comparison of absorption spectra of **1** and **3c**: the former absorbs at 617 nm with a ϵ of 150 M^{-1} cm^{-1}, and the latter, at 634 nm with a ϵ of 310 M^{-1} cm^{-1}. The contrast between **1** and **3c** can be further visualized from Figure 8, where the spectral changes of **1** upon titration of $Na_2$2-GP are shown. Similar spectral changes have been observed when **1**(*aq*) was titrated by other phosphate monoesters including HPO_4^{2-}, $PO_3(OPh)^{2-}$, α-D-Glc-1P, and DL-α-glycerol phosphate, and these plots are provided in the Supporting Information. A well-defined isosbestic point has been found in all titration plots, indicating an equilibrium between compound **1** and its phosphate monoester surrogate $Cu_2\{[18]ane\text{-}N_6\}(\mu\text{-}O\text{-}PO_3(OR))_2$ upon the addition of $(PO_3(OR))^{2-}$. Such an equilibrium can be further quantified through the determination of *apparent association constant* K_{rel} ($K_{rel} = K_{phosphate}/K_{acetate}$) by fitting the observed optical density (A) at 640 nm as a function of added $(PO_3(OR))^{2-}$ (molar concentration: R) according to the following relationship:[33]

$$A = A_1\{(K_{rel}C + K_{rel}R + 1) - [(K_{rel}C + K_{rel}R + 1)^2 - 4K_{rel}{}^2CR]^{1/2}\}/2K_{rel}C \quad (2)$$

where C and A_1 are respectively the initial concentration and the absorbance at 640 nm of **1**. As shown in Figure 9, the least-squares fit of changes in the optical density of **1** titrated by $Na_2$2-GP according to eq 2 gave an excellent correlation and an association constant of 3.4 (0.4) × 10^4.

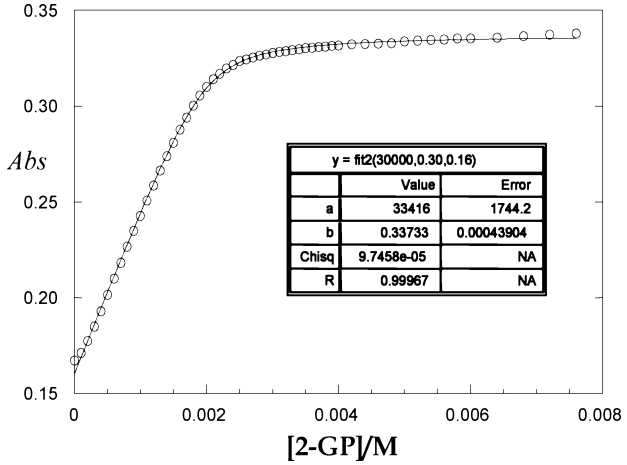

Figure 9. Changes of optical density (○) of a 1.0 mM solution of **1** titrated with $Na_2$2-GP, monitored at 640 nm. The theoretical fit is shown as a solid line.

Table 4. Anion Binding Constants of **1**

anion	K_{rel}[a] unbuffered	K_{rel}[a] buffered
HPO_4^{2-}	2.4 (0.7) × 10^4	4.3 (0.5) × 10^3
$(PhO)PO_3^{2-}$	1.1 (0.1) × 10^4	1.4 (0.1) × 10^3
$(HOCH_2)_2CHOPO_3^{2-}$	3.3 (0.2) × 10^4	2.9 (0.2) × 10^3
$(C_6H_{11}O_6)PO_3^{2-}$	1.7 (0.2) × 10^4	3.9 (0.2) × 10^3
$(HOCH_2CHOHCH_2O)PO_3^{2-}$	2.5 (0.4) × 10^4	2.5 (0.2) × 10^3
F^-	160 (25)	nd[b]
NO_3^-	20 (3)	nd[b]
HCO_3^-	160 (70)	nd[b]
PhO^-	nd[b]	nd[b]
HEPES	44 (4)	

[a] Apparent binding constants for an average of two titrations with less than 10% difference in the two runs. [b] Not detected within the experimental errors.

In addition to 2-GP, apparent association constants were thus determined for HPO_4^2, $PO_3(OPh)^{2-}$, α-D-Glc-1P, and DL-α-glycerol phosphate, and values are given in Table 4. In the case of HPO_4^{2-}, titration data (absorbance) beyond 1.4 equiv of HPO_4^{2-} were not used because of the occurrence

of precipitation resulting in an association constant with a fairly large error. The pH of the solution was found to vary within a narrow range of 6.0−8.0 for during all titrations. It is clear from Table 4 that the constants for all phosphate monoesters are of the same order of magnitude. Hence, the Cu_2{[18]ane-N_6} scaffold is *unselective* among different phosphate esters.

While the solution pH of the above-mentioned titrations was always in a narrow range of 6.0−8.0, it is desirable to assess the affinity of phosphate esters at the same pH, especially physiological pH. Thus, a second set of titrations were performed using the HEPES buffer to maintain the pH at 7.4, and the association constants determined from least-squares fitting are given also in Table 4 while the plots of data fittings are provided as the Supporting Information. It is surprising to find that the association constants have decreased by about 1 order of magnitude in comparison with those obtained from unbuffered titrations. It was subsequently determined that the HEPES buffer binds **1** weakly ($K_{rel} \sim 50$; titration curve and fit are shown in Figures S19 and S20 of the Supporting Information), presumably through the sulfonate group. Clearly, the competitive binding nature of the HEPES buffer reduced the phosphate ester binding to **1**. In fact, the competition between phosphate and sulfonate for the same recognition site has been long recognized in structural biology.[34] The weak but significant binding of HEPES to the Cu_2{[18]ane-N_6} moiety prompted us to examine the binding affinity to some nominally weak "coordinating" anions such as F^-, NO_3^-, HCO_3^-, and PhO^-. The association constants determined are shown in Table 4, and they are at least 2 orders of magnitude lower than those of phosphate esters. Clearly, Cu_2{[18]ane-N_6} is selective toward phosphate over other anions.

Conclusions

In summary, the novel Cu_2{[18]ane-N_6} core displays high affinities toward a broad spectrum of phosphate monoesters in aqueous solution at physiological pH and low affinities toward other common anions. Structural information about the complexes with phosphate monoesters is also relevant to metallophosphatases. Further improvement of the selectivity among different phosphate esters may be achieved by introducing functionalized side chains as C substituents of the Cu_2{[18]ane-N_6} core, a challenging task being pursued in our laboratory.

Experimental Section

Glycerol phosphate disodium salt pentahydrate, α-D-glucose-1-phosphate, and 1,4,7,10,13,16-hexaazacyclooctadecane trisulfate were purchased from Sigma-Aldrich. Sodium phenyl phosphate dibasic dehydrate, sodium phosphate, β-glycerol phosphate disodium salt pentahydrate, disodium DL-α-glycerophsphate, $Cu(OAc)_2$, $Cu(NO_3)_2$, phenol, NaF, $NaHCO_3$, $NaNO_3$, KPF_6, and K_2CO_3 were purchased from Fisher Scientific. Elemental analysis was performed by Atlantic Microlab (Norcross, GA). Aqueous spectroscopic titrations and electronic absorption spectra were performed on a Perkin-Elmer Lambda-900 UV−vis−near-IR spectrophotometer. The magnetic measurements were performed on a 7-T Quantum Design MPMS SQUID magnetometer. Measurements of magnetization as a function of temperature were performed from 5 to 300 K and in a 5000-G field. Approximately 15-mg samples were packed between cotton plugs, placed into gelatin capsules, cooled in zero applied field, and measured upon warming. Diamagnetic corrections were estimated based on Pascal's constants.

Synthesis of 1. An aqueous solution of 1.0 M KOH was added to a suspension of [18]aneN_6·$3H_2SO_4$ (0.20 g, 0.36 mmol) in 5 mL of H_2O until the solution turned clear (pH ∼8). To this clear solution was added $Cu(OAc)_2$·H_2O (0.15 g, 0.75 mmol) dissolved in 2 mL of H_2O to yield a solution of deep-blue color. Upon the addition of KPF_6 (0.27 g, 1.5 mmol), the solution was kept open to air under ambient conditions and yielded dark-blue crystals of **1** in 1 week [0.17 g, 61% based on $Cu(OAc)_2$]. Anal. Calcd (found) for **1** ($C_{16}H_{36}Cu_2F_{12}N_6O_4P_2$): C, 24.22 (23.98); H, 4.57 (4.35); N, 10.59 (10.32). UV−vis: λ_{max}, nm (ϵ, M^{-1} cm^{-1}) 263 (9060), 617 (150).

Synthesis of 2. To a suspension of [18]aneN_6·$3H_2SO_4$ (0.030 g, 0.054 mmol) in 3 mL of H_2O was added aqueous KOH (1 M) with stirring until the suspension turned clear. To this clear solution was added $Cu(NO_3)_2$·$3H_2O$ (0.027 g, 0.11 mmol) to yield a deep-blue solution. The addition of K_2CO_3 (0.021 g, 0.15 mmol) resulted in a solution of pH around 8, which, upon standing in air, yielded pale-blue plates (0.020 g, 60% based on [18]ane-N_6). Anal. Calcd (found) for **2**·$4.5H_2O$ ($C_{14}H_{39}Cu_2N_6O_{10.5}$): C, 28.67 (28.70); H, 6.70 (6.51); N, 14.33 (14.03). UV−vis: λ_{max}, nm (ϵ, $M^{-1}cm^{-1}$) 266 (3680), 630 (75).

Synthesis of 3a. To an aqueous solution of **1** (0.020 g, 0.025 mmol, 5 mL of H_2O) was added $(NH_4)_2HPO_4$ (0.010 g, 0.075 mmol) with vigorous stirring at ambient temperature. The resultant solution was evaporated in air for 1 week to yield **3a** as blue needles (0.015 g, 83% based on **1**). Anal. Calcd (found) for **3a**·$6H_2O$ ($C_{12}H_{44}N_6O_{14}P_2Cu_2$): C, 21.02 (21.08); H, 6.47 (6.34); N, 12.26 (12.25). UV−vis: λ_{max}, nm (ϵ, M^{-1} cm^{-1}) 263 (11 700), 634 (309).

Synthesis of 3b. To an aqueous solution of **1** (0.060 g, 0.075 mmol, 3 mL of H_2O) was added $Na_2C_6H_5PO_4$·$2H_2O$ (0.057 g, 0.225 mmol) with vigorous stirring at ambient temperature. Vapor diffusion of acetone into the resultant solution resulted in **3b** as blue rectangular crystals in 1 week (0.035 g, 64% based on **1**). Anal. Calcd (found) for **3b**·$6H_2O$ ($C_{24}H_{52}Cu_2N_6O_{14}P_2$): C, 34.41 (34.26); H, 6.26 (6.28); N, 10.03 (10.05). UV−vis: λ_{max}, nm (ϵ, M^{-1} cm^{-1}) 263 (11 700), 630 (250).

Synthesis of 3c. To an aqueous solution of **1** (0.60 g, 0.075 mmol, 3 mL of H_2O) was added $Na_2CH(CH_2OH)_2PO_4$·$5H_2O$ (0.69 g, 0.23 mmol) with vigorous stirring at ambient temperature. The resultant solution was layered with acetone to afford deep-blue crystals of **3c** (0.44 g, 72% based on **1**). Anal. Calcd (found) for

(32) Kato, M.; Sah, A. K.; Tanase, T.; Mikuriya, M. *Eur. J. Inorg. Chem.* **2006**, 2504. Youngme, S.; Phatchimkun, J.; Suksangpanya, U.; Pakawatchai, C.; van Albada, G. A.; Reedijk, J. *Inorg. Chem. Commun.* **2005**, *8*, 882. Doyle, R. P.; Kruger, P. E.; Moubaraki, B.; Murray, K. S.; Nieuwenhuyzen, M. *Dalton Trans.* **2003**, 4230. Moreno, Y.; Vega, A.; Ushak, S.; Baggio, R.; Pena, O.; Le Fur, E.; Pivan, J. Y.; Spodine, E. *J. Mater. Chem.* **2003**, *13*, 2381. Spiccia, L.; Graham, B.; Hearn, M. T. W.; Lazarev, G.; Moubaraki, B.; Murray, K. S.; Tiekink, E. R. T. *Dalton Trans.* **1997**, 4089.

(33) Kral, V.; Furuta, H.; Shreder, K.; Lynch, V.; Sessler, J. L. *J. Am. Chem. Soc.* **1996**, *118*, 1595.

(34) Kanyo, Z. F.; Christianson, D. W. *J. Biol. Chem.* **1991**, *266*, 4264.

(35) *SAINT V 6.035 Software for the CCD Detector System*; Bruker-AXS Inc.: Madison, WI, 1999.

(36) *SHELXTL 5.03 (WINDOW-NT Version), Program library for Structure Solution and Molecular Graphics*; Bruker-AXS Inc.: Madison, WI, 1998.

Table 5. Crystal Data and Structural Refinement for Compounds **1**−**3**

	1	**2**·10H_2O	**3a**·8H_2O	**3b**·6H_2O	**3c**·5H_2O	**3d**·12H_2O
chemical formula	$C_{16}H_{36}F_{12}N_6O_4P_2Cu_2$	$C_{14}H_{50}N_6O_{16}Cu_2$	$C_{12}H_{48}N_6O_{16}P_2Cu_2$	$C_{24}H_{52}N_6O_{14}P_2Cu_2$	$C_{18}H_{54}N_6O_{17}P_2Cu_2$	$C_{24}H_{76}N_6O_{30}P_2Cu_2$
fw	793.5	685.7	721.6	837.7	815.7	1117.9
space group	*C*2 (No. 5)	$P2_1/n$ (No. 14)	$P2_1/c$ (No. 14)	*Pbca* (No. 61)	*Cc* (No. 9)	$P3_1$ (No. 144)
a, Å	16.313(2)	10.247(1)	7.400(1)	11.485(1)	23.187(8)	14.4510(9)
b, Å	9.823(1)	7.376(1)	10.710(1)	16.654(1)	8.135(2)	
c, Å	9.306(1)	19.031(2)	17.683(2)	18.256(1)	18.158(7)	20.651(2)
β, deg	97.010(2)	96.425(2)	99.086(2)		106.72(2)	
V, Å^3	1480.0(2)	1429.4(2)	1383.8(2)	3491.6(4)	3280(2)	3734.9(5)
Z	2	2	2	4	4	3
T, °C	27(2)	27(2)	27(2)	27(2)	27(2)	27(2)
λ(Mo Kα), Å	0.71073	0.71073	0.71073	0.71073	0.71073	0.71073
ρ_{calc}, g cm^{-3}	1.781	1.593	1.732	1.594	1.652	1.491
μ, mm^{-1}	1.656	1.566	1.732	1.382	1.474	1.012
R1	0.048	0.045	0.046	0.050	0.063	0.072
wR2	0.133	0.121	0.117	0.123	0.159	0.180

3c·4H_2O ($C_{18}H_{52}Cu_2N_6O_{16}P_2$): C, 27.10 (27.43); N, 10.54 (10.25); H, 6.57 (6.34). UV−vis: λ_{max}, nm (ϵ, M^{-1} cm^{-1}): 266 (7300), 630 (240).

Synthesis of 3d. To a suspension of [18]ane-N_6·3H_2SO_4 (0.030 g, 0.054 mmol, 2 mL of H_2O) was added a 1.0 M KOH solution until the solution became transparent. To this solution was added $Cu(NO_3)_2$·3H_2O (0.017 g, 0.11 mmol, 2 mL of H_2O) to yield a solution of deep-blue color, which was followed by the addition of $K_2C_6H_{11}PO_9$·2H_2O (0.080 g, 0.22 mmol) with vigorous stirring. Vapor diffusion of methanol into the resultant blue solution yielded **3d** as blue crystals in 1 week (0.020 g, 30% based on [18]ane-N_6). Anal. Calcd (found) for **3d**·9H_2O ($C_{24}H_{70}Cu_2N_6O_{27}P_2$): C, 27.10 (27.03); H, 6.63 (6.26); N, 7.90 (7.83). UV−vis: λ_{max}, nm (ϵ, M^{-1} cm^{-1}): 263 (10 300), 627 (270).

Titrations. Spectroscopic titrations were performed with a cuvette of 1-cm optical path containing 3.0 mL of a 1 mM aqueous solution of {[18]aneN_6Cu_2(μ-O-OAc)$_2$}(PF_6)$_2$. Aliquots of a 100 mM aqueous solution of the corresponding phosphate monoester were subsequently added, and the resultant solution was allowed to equilibrate for 5 min before the spectrum was recorded. Buffered experiments were performed in solutions that are 5 mM HEPES and maintained at pH 7.40. All titrations were performed at 22.5 °C.

Structure Determination. Single crystals were obtained as previously stated. X-ray intensity data were measured at 300 K on a Bruker SMART1000 CCD-based X-ray diffractometer system using Mo Kα (λ = 0.710 73 Å). Crystals used for data collection were cemented to a quartz fiber with epoxy glue. Data were measured using ω scans of 0.3°/frame for 10 s for compounds **1**−**3** (Table 5) so that a hemisphere (1271 frames) was collected. The frames were integrated with the Bruker *SAINT* software package[35] using a narrow-frame integration algorithm, which also corrects for the Lorentz and polarization effects. Absorption corrections were applied using *SADABS*.[35]

Structures were solved and refined using the Bruker *SHELXTL* (version 5.1) software package. Positions of all non-H atoms were revealed by direct methods. All non-H atoms are anisotropic, and the H atoms were put in calculated positions and riding mode.[36] Each structure was refined to convergence by a least-squares method on F^2, *SHELXL-93*, incorporated in *SHELXTL* PC version 5.03. Crystallographic data are given in Table 2.

Acknowledgment. This work was supported, in part, by the Army Research Office (Grant DAAD 190110708 to T.R.) and the Office of Naval Research (Grant N00014-03-1-0531 to T.R.). G.T.Y. thanks the National Science Foundation (Grant CHE-023488) and Virginia Tech (ASPIRES program) for the funding of SQUID. We are thankful for the early contribution of N. Martin.

Supporting Information Available: Experimental details of spectral titration of compound **1** by both phosphate monoesters and other anions and crystallographic data (CIF) of compounds **1**−**3**. This material is available free of charge via the Internet at http://pubs.acs.org.

IC0611140